

RESEARCH PAPER

Harvesting Power Through Random Vibrations of Aerospace Vehicles from Nanostructured La-Pb(Ni_{1/3}Sb_{2/3}) - PbZrTiO₃ Ferroelectric Ceramics

H.H. Kumar^{#,*}, C.M. Lonkar[#], and Balasubramanian K.[!]

[#]PZT Center, Armament Research and Development Establishment, Pune - 411 021, India

[!]Defence Institute of Advanced Technology (Deemed University), Pune - 411 025, India

*E-mail: hhkumar123@gmail.com

ABSTRACT

Synthesis by mechanochemical activation route and optimisation for power harvesting properties of nano-structured Pb_{0.98}La_{0.02}(NiSb)_{0.05}[(Zr_{0.52}Ti_{0.48})_{0.995}]_{0.95}O₃ [La-PNS-PZT] ferroelectric ceramic composition has been carried out and reported here for the first time. Progressive perovskite phase formation during mechanical activation from 5 h to 40 h followed by reactive sintering was analysed from X-Ray diffraction analysis. Noticeable formation of perovskite phase after 10 h of milling and further its completion in successive reactive sintering was observed. Particle morphology of the 10 h activated nano-La-PNS-PZT powder analysed by high resolution transmission electron microscope indicated average particle size (d_{50}) of about 24 nm. Microstructural studies of samples reactively sintered at 1220 °C were performed by field emission scanning electron microscopy for powders activated for various durations, indicated the compact microstructure for 10 h activation which resulted in optimum piezoelectric properties viz. piezoelectric charge coefficient ($d_{33} = 449 \times 10^{-12}$ C/N), piezoelectric voltage coefficient ($g_{33} = 32 \times 10^{-3}$ m-V/N), Figure of merit for power harvesting (14.4×10^{-12} V-m-C/N²) accompanied by excellent stability of permittivity in the range -50 °C to 100 °C. The output voltage obtained from simulated random vibrations of aerospace vehicles at various power spectrum density values, measures about 3.0 mV output across resistance of 1 kΩ indicating suitability of composition for harvesting the power from aerospace vehicle vibrations .

Keywords: Nano- La-PNS-PZT, mechanical activation, power harvesting, random vibration test, Aerospace vehicle vibrations

1. INTRODUCTION

PZT based piezoceramics are electromechanical energy converters, are suitable for sensors, actuators¹⁻⁴ and power harvesting applications⁵⁻⁸ in civil and defence sectors⁹. PZT compounds crystallize in ABO₃ type perovskite structure in which 'A' is a large divalent Pb²⁺ cation occupies the corner of the unit cell. Zr⁴⁺ and Ti⁴⁺ are small tetravalent cations occupy the ferroelectrically affected 'B' position at the displaced centre while O²⁻ is the face centered anion. Due to minimal potential energy considerations, positive and negative charge sites do not coincide and thus form the dipole⁸. Formation of spontaneous dipole due to separation of positive and negative charge centres and further alteration in this separation due to application of stress is the origin of piezoelectricity in perovskite structured PZT compositions⁸. Compositions with superior piezoelectric charge coefficient (d_{33}) are suitable for actuator applications^{10,11} while higher values of piezoelectric voltage coefficients lead to generation of higher voltages and hence find suitability for sensor¹² and power harvesting applications^{5-8, 13,14}.

PZT compositions can be obtained by wet chemical methods like sol-gel, co-precipitation, hydrothermal etc. and dry methods like solid state route¹⁵⁻¹⁷ or mechanical activation (MA) processes¹⁸ for nano crystalline ceramics. Mechanical

activation process employs high energy ball mill (HEBM) in which raw material powders are milled intimately by tungsten carbide balls. Due to combined effect of mechanical energy and temperature in the HEBM¹⁸ particles fused together and ruptured continuously¹⁹. This initiates the chemical reaction among raw material powders along with reduction in particle size to nanometre regime, thereby evading the calcination stage of conventional mixed oxide route²⁰. Nanomaterials attracted researchers since it creates a possibility of improving the properties due to variation in crystallite size^{1,18}. MA process was employed around 1966 by Benjamin for formation of oxide dispersed metal alloys for structural applications^{19,21}. Since then, it has been widely used by several researchers for preparation of nano PZT based materials. Practically, possibility of contamination of tungsten carbide increases due to availability of larger surface area due to large reduction in particle size and formation of newer surface area for larger milling times¹⁹. However, this can be overcome by carrying out MA for reduced durations followed by 'Reactive Sintering' to further complete the solid state reaction.

Pb(Ni_{1/3}Sb_{2/3})O₃-PbZrTiO₃, abbreviated as PNS-PZT, is a solid solution of complex perovskite of type Pb(B'_{1/3}B''_{2/3})O₃-Pb(B)O₃ have been studied by some of the researchers around its morphotropic phase boundary (MPB) of PNS-PZT (i.e. 0.12 PNS -0.40 PZ -0.48 PT) for various compositional

modifications, processing parameters and their effects on dielectric and piezoelectric properties²²⁻²⁶. The authors of the present work, have also investigated and reported a novelty of a lanthanum doped PNS-PZT compositions [La-PNS-PZT], at MPB of PZT and reported for various properties suitable for power harvesting^{2,7}, underwater sensor⁹ and actuator applications^{7,27} during their earlier studies. All these studies were restricted to the compositional powders in micro-meter regime.

In the present study, authors synthesised Nano-La-PNS-PZT composition by columbite precursor method, followed by mechanical activation using High Energy Ball Mill. Mechanical activation induced structural effects were correlated with the piezoelectric properties and their optimisation for power harvesting applications. Another goal was to explore the stability of properties over the temperature and suitability of the compositions for power harvesting through random vibrations of aerospace vehicles.

2. EXPERIMENTAL

Nanostructured composition $\text{Pb}_{0.98}\text{La}_{0.02}(\text{NiSb})_{0.05}[(\text{Zr}_{0.52}\text{Ti}_{0.48})_{0.995}]_{0.95}\text{O}_3$ of the present study, was synthesised from oxides of elements in the powder form using PbO (Waldies Ltd., India, 99.65%), ZrO_2 (Indian Rare Earths Ltd, India, 99.70 %), TiO_2 (Travancore Titanium Products, India, 98.50 %), NiO (Acros, India 97 %), Sb_2O_5 (Loba Chemie, India 99 %) and La_2O_3 (Indian Rare Earths Ltd., India, 99.99%) by mechanical activation using high energy ball milling process. Pyrochlore-free single perovskite phase La-PNS-PZT ceramic was obtained by synthesising B site precursor NiSb_2O_6 [NS] by solid state route in first stage, followed by mechanical activation of NS with remaining oxides using high energy ball mill (Retch, model-PM 400). The powder was activated for 5 h, 10 h, 20 h, 30 h, and 40 h at 300 rpm. We have used ball to powder weight ratio (BPR) as 13:1. The progressive transition of starting oxide powders into desired composition during mechanical activation were investigated from X-ray diffraction patterns recorded for position 2θ from 20° to 60° , step size 0.02° , scan speed 0.1 s/step using $\text{CuK}\alpha$ line ($\lambda=1.54 \text{ \AA}$) (D8 Advance, Bruker, Germany). Effects of activation on microstructure were analysed using HRTEM (TECNAI G2, FEI). Further, powder was compacted uniaxially to form pellets of density 4.8 g/cc. The pellets were reactively sintered in lead rich atmosphere in covered alumina crucibles at 1220°C . Surface morphology of polished and chemically etched sintered samples was analysed using FESEM (Sigma, ZEISS, Germany). Lapped pellets (dia. 10 mm x thick. 1 mm) were electroded by fired on silver and poled by applying DC field of 30 kV/cm at 100°C for 30 min in silicon oil bath. Dielectric properties were measured at 1 kHz using LCR High Tester (HIOKI-3532, Japan). Piezoelectric charge coefficient (d_{33}) was measured at 100 Hz using piezo d_{33} Meter (PM 300 Piezo Test, UK). Piezoelectric voltage coefficient (g_{33}) and figure of merit for power harvesting (FoM_{ph}) were calculated using standard mathematical relations^{5,7,22}. Temperature stability of dielectric constant was evaluated in the temperature range between -50°C and $+340^\circ\text{C}$ using dielectric analyser (Novatherm Quotro, Novocontrol GmbH).

In this study, authors have assumed the specifications generated by Kumar²⁸, *et al.* Electrical output voltage of test samples in response to simulated random vibrations of aerospace / launch vehicle have been acquired for various power spectrum density, using vibration shaker (Saraswati Dynamics) controlled through vibration controller VR9500 of Vibration Research Corporation. The time domain data is analysed by Inverse Fourier Transform in frequency domain and correlated to power harvesting and microstructure of reactively sintered samples.

3. RESULTS AND DISCUSSIONS

3.1 Crystallographic Analysis

X-ray diffraction patterns for position 2θ from 20° to 60° for Mechanically Activated powder for 5 h to 40 h denoted respectively, by MA-5 to MA-40 and that of corresponding Reactively Sintered samples denoted respectively by RS-5 to RS-40 are as shown in Fig. 1. Patterns for powders demonstrate the progressive transition of oxides into desired perovskite phase. Subsequently, reactive sintering of the same shows the transformation of powders into pure perovskite phase for entire range of activation time. With increasing the activation time, crystallinity improved indicated by reduction in peak widths. Though 5 h milled powder show existence of perovskite phase, it also shows the existence of mixture of starting powders along with traces of PbTiO_3 ^{29,30} and PbZrO_3 ³¹. Increasing the milling time to 10 h, mechanically activated solid state reaction is advanced largely, leading to formation of perovskite phase to greater extent indicated by rise in peak intensity of perovskite planes^{7,22} and reduction in peaks for starting components. Further increasing the milling duration to 20 h and 30 h, improvement of solid state reaction for formation of La-PNS-PZT in perovskite phase was noticed. For 40 h milling time,

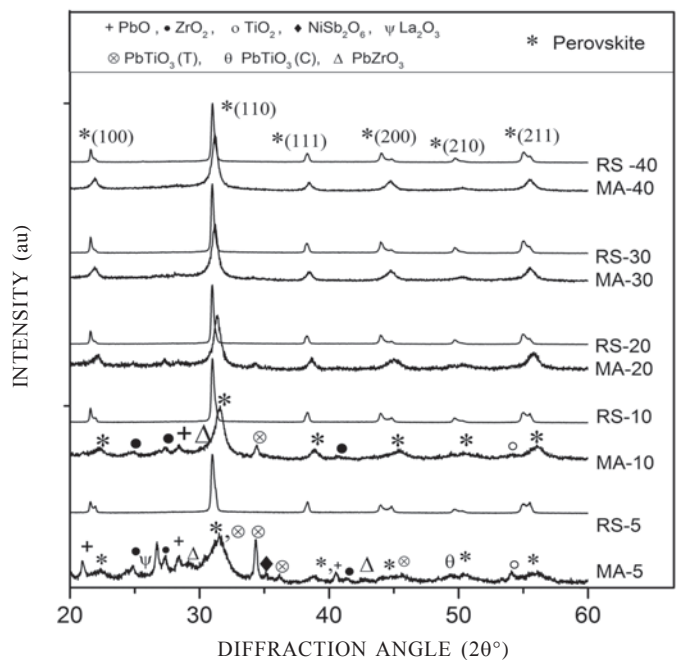


Figure 1. XRD pattern for mechanically activated (MA) Nano-crystalline powder samples and reactively sintered samples (RS).

entire quantity of starting materials are converted into desired La-PNS-PZT composition, which is evident from peaks for single perovskite phase. Though the unreacted starting oxides were present in the activated powders, they get transformed into desired perovskite phase on sintering as indicated by respective XRD patterns (RS-5 to RS-40) along with increase in unit cell dimensions evidenced by shifting of corresponding peaks on lower side. Furthermore, reactively sintered compositions were free from pyrochlore phase ($\text{Pb}_2\text{Sb}_2\text{O}_7$) as the associated peaks were absent in the diffraction pattern^{23,32,33}.

3.2 Microstructural Analysis

Figure 2 is representative HRTEM of particle morphology of powder obtained by mechanical activation for 10 h (MA-10). Along with several distinct spherical particles, few aggregates were also noticed, as normally observed³⁴. Average particle size (d_{50}) achieved is about 22 nm - 25 nm for this activation time. This shows that 10 h milling is sufficient for chemical reactions to take place among the constituent oxides along with reduction in particle size to nano-meter scale.

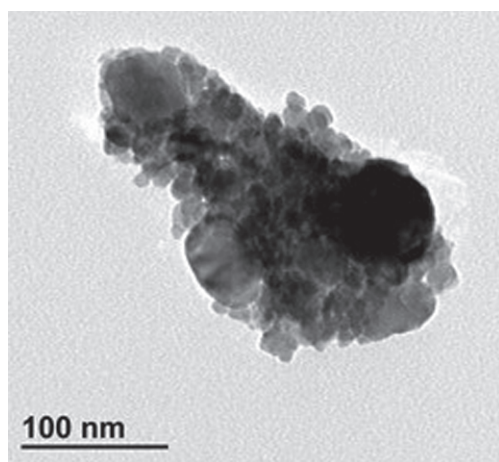


Figure 2. TEM of Nano-crystalline powder mechanically activated for 10 h (MA-10).

Figure 3 (a)-(e) shows the effect of mechanical activation on microstructure of the samples reactively sintered at 1220°C. The average grain size (d_{50}) was measured using liner intercept method. Increasing the activation time from 5 h to 10 h, d_{50} decreased and further it remained practically uniform till 30 h activation and increased noticeably at 40 h. Grains with assorted polygons accompanied by wide range of size distribution ($\leq 12 \mu\text{m}$) were observed at 5 h activation indicating insufficient time for activation and mixing (Fig. 3(a)). As shown in Fig. 3(b), the grain morphology changed significantly on increasing the activation to 10 h. Closely packed, hexagonal shaped grains with straight edges were observed representing the complete grain growth. Size distribution of grains was also narrow. Reduction in porosity and porosity at triple grain point was observed which indicated better sinterability at 1220 °C for 10 h activation time. Increasing the activation time to 20 h and 30 h, grain size remained practically unchanged but compactness reduced which lead to appearance of few ovular shaped grains. Grain morphology drastically changed and

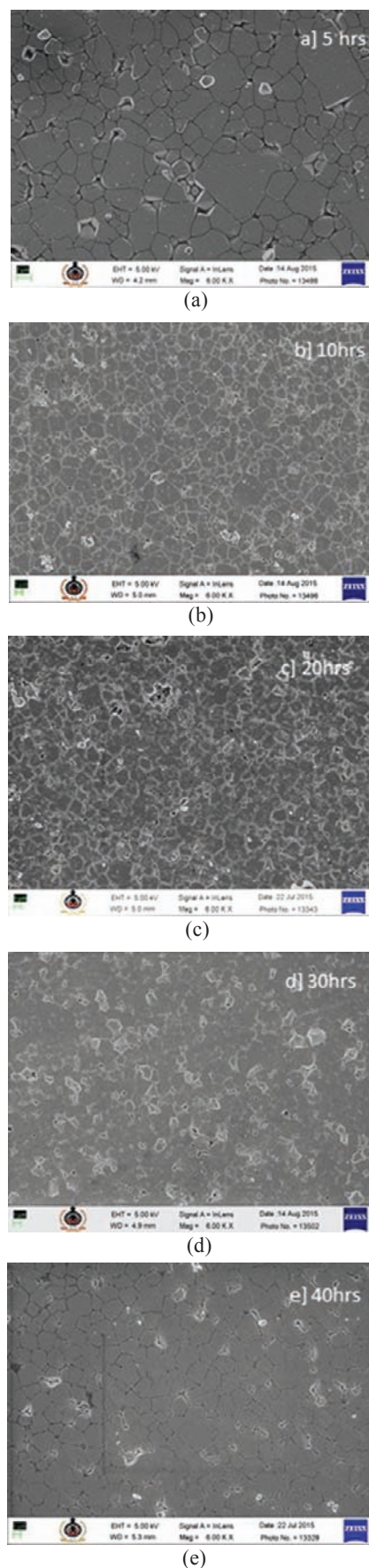


Figure 3. SEM of Reactively Sintered samples obtained from powders mechanically activated for (a) 5 h, (b) 10 h, (c) 20 h, (d) 30 h, and (e) 40 h.

multifarious sized and shaped grains were observed for 40 h activation, though microstructure is seen to be compact. The average grain size (d_{50}) measured was 3.46 μm , 1.65 μm , 1.67 μm , 1.76 μm , and 2.37 μm for the samples fabricated from powders mechanically activated for 5 h, 10 h, 20 h, 30 h, and 40 h respectively and reactively sintered at 1220 $^{\circ}\text{C}$.

3.3 Piezoelectric Properties for Power Harvesting Applications

Effects of activation time on various dielectric and piezoelectric properties are listed in Table 1. Values of piezoelectric charge coefficient (d_{33}) obtained for 10 h of milling (449 pC/N) and 20 h of milling (457 pC/N) are improved and comparable. Superior values are attributed to the increased polarisability and compact microstructure²² having optimum grain size³⁵⁻³⁸, as noticed in SEM micrographs for these activation durations. Increasing the activation time, it reduced to 229 pC/N (40 h). Piezoelectric voltage coefficient (g_{33}) and figure of Merit for power harvesting (FoM_{ph}) were calculated using general equations given in the literature. g_{33} values are influence by d_{33} and permittivity. Optimum value of g_{33} obtained at 10 h activation time attributed to better d_{33} and lower permittivity values (1585). Better value of d_{33} and optimum value of g_{33} resulted into optimum FoM_{ph} ^{5,6,8,13,14} indicating the suitability of the composition activated for 10 h (MA-10) for power harvesting applications.

Table 1. Effect of Mechanical Activation time on various dielectric and piezoelectric properties

MA duration (h)	$d_{33}(\times 10^{-12} \text{ C/N})$	K_3^T	$g_{33}(\times 10^{-3} \text{ m-V/N})$	$\text{FoM}_{\text{ph}} d_{33}^* g_{33} (\times 10^{-12} \text{ V-m-C/N}^2)$
5	340	1592	24.1	8.2
10	449	1585	32.0	14.4
20	457	1762	29.3	13.4
30	420	1725	27.5	11.6
40	229	1437	18.0	4.1

3.4 Temperature Dependence and Stability of Properties

Figure 4 shows temperature dependence of permittivity and phase transition behavior investigated at 1 kHz for MA-10 samples. It was observed that, the permittivity remained almost unaltered till 150 $^{\circ}\text{C}$. A small bump (T_{RT}) observed near 165 $^{\circ}\text{C}$, refers to ferroelectric rhombohedral (F_R) to ferroelectric tetragonal (F_T) phase transition^{39,40}. Further increasing the temperature, ferroelectric (F_E) to paraelectric (P_c) phase transition was observed at 290 $^{\circ}\text{C}$ indicated by sharp peak (T_c). It is interesting to note the excellent temperature stability of permittivity of the composition over the temperature range of -50 $^{\circ}\text{C}$ to 100 $^{\circ}\text{C}$ to which the aerospace / launch vehicles are generally subjected to during the operation.

3.5 Power Harvestability in Response to Random Vibrations

As shown in Fig. 5, components in the form of round discs (Φ 9.8 mm x thk 1.1 mm) were fixed on fixture using

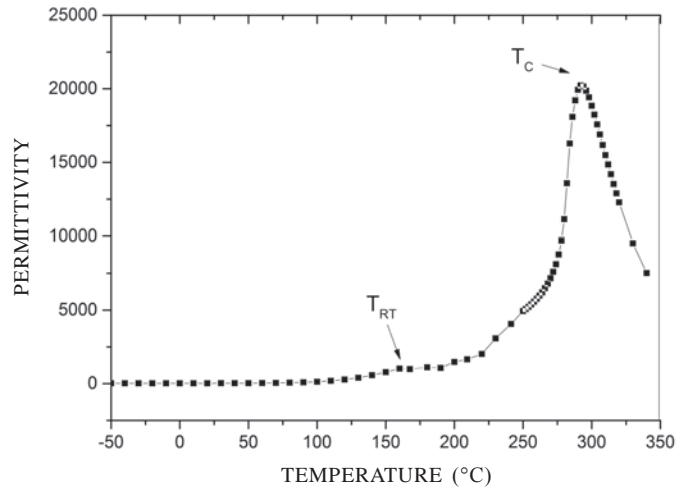


Figure 4. Temperature dependence of permittivity and phase transition behaviour.

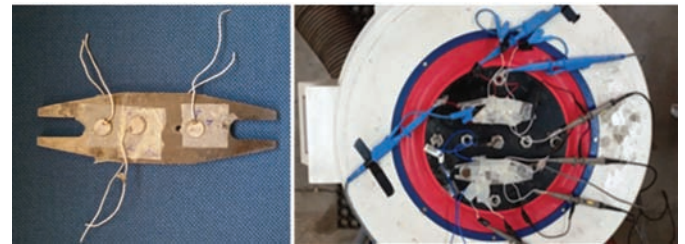


Figure 5. Fixture with components and vibration bench.

petro-wax (PCB Piezotronics) and the fixture was mounted by steel bolts on vibration bench.

Power spectrum density (PSD) values of random vibrations of aerospace vehicles along Z-axis as recorded by Manoj²⁸, *et al.* were used as input to MA-10 piezo discs in our experimental work (Fig. 6). Components were allowed to freely vibrate along Z-axis along with the bench and the inertia of the disc is responsible for generator action in response to random vibrations.

Figure 7 shows the output voltage across load resistances between 1 k Ω - 7 k Ω of MA-10 piezo discs in response to

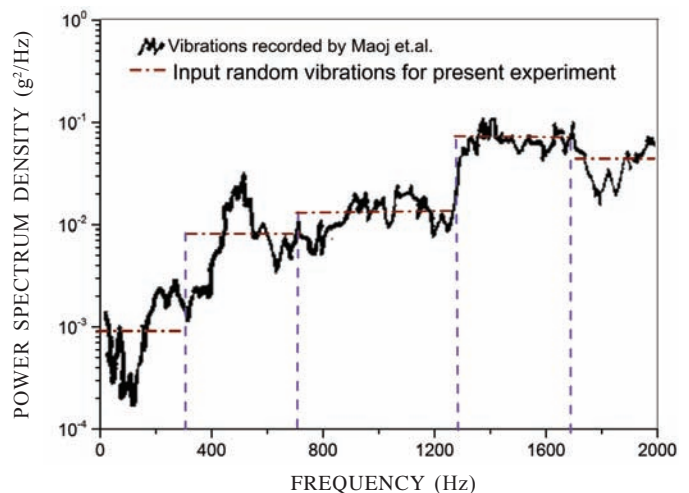


Figure 6. Random vibrations of aerospace vehicles along Z-axis²⁸.

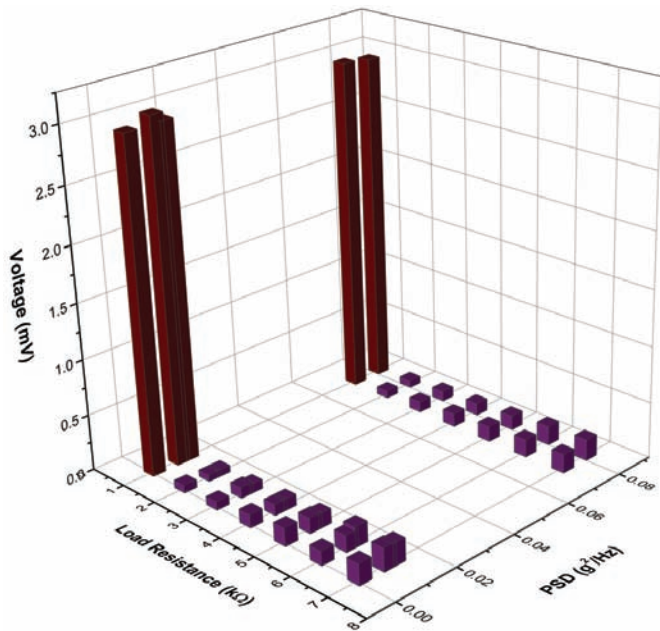


Figure 7. Voltage output at random vibrations in terms of PSD and load resistance.

random vibrations in terms of PSD. Maximum output voltage was obtained at 1 k Ω load resistance for the entire range of random vibrations applied in the experiment. Maximum output at this resistance is attributed to the matching of electrical impedance⁴¹⁻⁴⁴ of MA-10 piezo discs under the present experimental conditions. Moreover, the excellent uniformity of the output voltage (2.98 ± 0.04 mV) was observed. However the electrical output can be improved substantially by converting the components into vibration based devices like bimorph type cantilever modelled with the help of FEA software.

4. CONCLUSIONS

Pyrochlore free, $\text{Pb}_{0.98}\text{La}_{0.02}(\text{NiSb})_{0.05}[(\text{Zr}_{0.52}\text{Ti}_{0.48})_{0.995}]_{0.95}\text{O}_3$ [La-PNS-PZT] composition, suitable for power harvesting has been synthesised using mechanochemical activation route. Progressive perovskite phase formation during mechanical activation and reactive sintering, analysed from XRD data, indicated the noticeable evidence of formation of perovskite phase after 10 h of activation and its completion during reactive sintering. HRTEM images shows the evidence of nanostructured particle size of the composition. Microstructural studies of samples carried out by FESEM indicated the compact microstructure for 10 h activation which resulted in optimum power harvesting piezoelectric properties accompanied by excellent stability of permittivity upto 100 $^{\circ}\text{C}$. The electrical output evaluated in response to simulated random vibrations of aerospace vehicles at various power spectrum density values, measures at 3.0 mV output across the matched load resistance of 1 k Ω indicated suitability of composition for harvesting the power from vibrations of aerospace vehicles .

REFERENCES

1. Mahmud, I.; Ur, S.C. & Yoon, M.S. Effect of high-energy milling process on microstructure and piezoelectric/dielectric properties of $0.99\text{Pb}(\text{Zr}_{0.53}\text{Ti}_{0.47})\text{O}_3-0.01\text{BiYO}_3$

ceramic for piezoelectric energy harvesting devices. *Electron. Mater. Lett.*, 2014, **10**(1), 223-228.

doi: 10.1007/s13391-013-3060-z

2. Lonkar, C.M.; Kharat, D.K.; Kumar, H.H.; Prasad, S. & Balasubramanian, K. Effect of sintering time on dielectric and piezoelectric properties of lanthanum doped $\text{Pb}(\text{Ni}_{1/3}\text{Sb}_{2/3})-\text{PbZrTiO}_3$ ferroelectric ceramics. *Def. Sci. J.*, 2013, **63**(4), 418-422.
doi: 10.14429/dsj.63.4866
3. Mahmud, I.; Ur, S.C. & Yoon, M.S. Piezoelectric materials of $(1-x)\text{Pb}(\text{Zr}_{0.53}\text{Ti}_{0.47})\text{O}_3-x\text{Bi}(\text{Y}_{0.7}\text{Fe}_{0.3})\text{O}_3$ for energy-harvesting devices. *Microelectron. Eng.*, 2014, **126**(C), 71-78.
doi: 10.1016/j.mee.2014.06.024
4. Haertling, G.H. Ferroelectric ceramics: History and technology. *J. Am. Ceram. Soc.*, 1999, **82**(4), 797-818.
doi: 10.1111/j.1151-2916.1999.tb01840.x
5. Maurya, D.; Yongke Yan & Priya, S. Piezoelectric materials for energy harvesting. In *Advanced Materials for Clean Energy*, Qiang Xu, Tetsuhiko Kobayashi (Ed), CRC Press, FL, USA, 2015.
doi: 10.1201/b18287-6
6. Kim, H.; Priya, S.; Uchino, K. & Newnham, R. Piezoelectric energy harvesting under high pre-stressed cyclic vibrations. *J. Electroceram.* 2005, **15**(1), 27-34.
doi: 10.1007/s10832-005-0897-z
7. Lonkar, C.M.; Kharat, D.K.; Kumar, H.H.; Prasad, S. & Balasubramanian, K. Effect of La on piezoelectric properties of $\text{Pb}(\text{Ni}_{1/3}\text{Sb}_{2/3})\text{O}_3-\text{Pb}(\text{ZrTi})\text{O}_3$ ferroelectric ceramics, *J. Mater. Sci. Mater. Electron*, 2013, **24**(1), 411-417.
doi: 10.1007/s10854-012-0765-y
8. Moulson, A.J. & Herbert, M. *Electroceramics materials properties applications*. (2nd edition), John Wiley & Sons Ltd, London, 2003, pp. 384
9. Lonkar, C.M.; Kharat, D.K.; Kumar, H.H.; Prasad, S.; Balasubramanian, K. & Prasad, N. Study of $\text{Pb}(\text{Ni}_{1/3}\text{Sb}_{2/3})\text{O}_3-\text{PbZrTiO}_3$ ceramic sensors for underwater transducer application. *Def. Sci. J.*, 2012, **62**(4), 269-273.
doi: 10.14429/dsj.62.1718
10. Jordan, T.L. & Ounaies, Z. Piezoelectric ceramics characterization. ICASE Report No. 2001-2028, 2001, NASA/CR-2001-211225.
11. Zhou, D; Kamlah, M. & Munz, D. Effects of uniaxial prestress on the ferroelectric hysteretic response of soft PZT. *J. Eur. Ceram.*, 2005, **25**(4), 425-432.
doi: 10.1016/j.jeurceramsoc.2004.01.016
12. Tressler, J.F.; Sedat, A. & Newnham, R. Piezoelectric Sensors and Sensor materials. *J. Electroceram.* 1998, **2**(4), 257-271.
doi: 10.1023/A:1009926623551
13. Kulkarni, V.; Mrad, B. R.; Prasad, E. & Nemana, S. A shear-mode piezoceramic device for energy harvesting applications. In *International Workshop Smart Materials, Structures and NDT in Aerospace Conference Canada 2011*, November 2 - 4, 2011, Montreal, Quebec, Canada.
14. Priya, S.; Taneja, R.; Myers, R. & Islam, R. Piezoelectric energy harvesting using bulk transducers in piezoelectric

- and acoustic materials for transducer applications, Springer Science+Business Media, LLC, 2008.
15. Prabu, M.; Shameeban, I. N.; Gobalankrishnan, S. & Murthy, C. Electrical and ferroelectric properties of undoped and La-doped PZT (52/48) electroceramics synthesized by sol-gel method. *J. Alloys Compd.*, 2013, **551**, 200–207.
doi: 10.1016/j.jallcom.2012.09.095
 16. Chang, T.I.; Huang, J.L.; Lin, H.P.; Wang, S.C.; Lu, H.H.; Wu, L. & Lin, J.F. Effect of drying temperature on structure, phase transformation of sol-gel-derived lead zirconatetitanate powders. *J. Alloys Compd.*, 2006, **414**(1-2), 224–229.
doi: 10.1016/j.jallcom.2005.07.011
 17. Wang, S.F.; Wang, Y.R.; Mahalingam, T.; Chu, J.P. & Lin K.U. Characterization of hydrothermally synthesized lead zirconatetitanate (PZT) ceramics. *Mater. Chem. Phys.* 2004, **87**(1), 53–58.
doi: 10.1016/j.matchemphys.2004.04.009
 18. Miclea, C.; Tanasoiu, C.; Gheorghiu, A.; Miclea, C.F. & Tanasoiu, V. Synthesis and piezoelectric properties of nanocrystalline pzt-based ceramics prepared by high energy ball milling process, *J. Mater. Sci.*, 2004, **39**(16-17), 5431-5434.
doi: 10.1023/B:JMSS.0000039260.82430.f9
 19. Suryanarayana, C.; Inov, E. & Boldyrev, V.V. The science and technology of mechanical alloying. *Mater. Sci. Engg-A*.2001, **304-306**, 151-158.
doi: 10.1016/S0921-5093(00)01465-9
 20. Lee, S.E.; Xue, J.M.; Wan D.M. & Wang, J. Effects of mechanical activation on the sintering and dielectric properties of oxide-derived PZT. *Acta. Mater.*, 1999, **47**(9), 2633-2639.
doi: 10.1016/S1359-6454(99)00141-X
 21. Kong, L. B.; Zhang, T. S.; Ma, J. & Boey, F. Y. C. Progress in synthesis of ferroelectric ceramic materials via high-energy mechanochemical technique. *Prog. Mater. Sci.*, 2008, **53**(2), 207-322.
doi: 10.1016/j.pmatsci.2007.05.001
 22. Wang, M.C.; Haung, M.S.; Tze-Shoeng & Nan-Chung, W. Sintering and piezoelectric properties of $\text{Pb}(\text{Ni}_{1/3}\text{Sb}_{2/3})\text{O}_3\text{-PbZrO}_3\text{-PbTiO}_3$ ferroelectric ceramics. *J. Mater. Sci.*, 2002, **37**(3), 663-668.
doi: 10.1023/A:1013746414023
 23. Wang, M.C.; Huang, M.S. & Chung, N. W. Effects of $30\text{B}_2\text{O}_3\text{-}25\text{BiO}_3\text{-}45\text{CdO}$ glass addition on sintering of $12\text{Pb}(\text{Ni}_{1/3}\text{Sb}_{2/3})\text{O}_3\text{-}40\text{PbZrO}_3\text{-}48\text{PbTiO}_3$ piezoelectric ceramics, *J. Eur. Ceram. Soc.* 2001, **21**(6), 695-701.
doi: 10.1016/S0955-2219(00)00272-7
 24. Zahi, S.; Bouaziz, R. & Abdesslem, N. A Dielectric and piezoelectric properties of $\text{PbZrO}_3\text{-PbTiO}_3\text{-Pb}(\text{Ni}_{1/3}\text{Sb}_{2/3})\text{O}_3$ ferroelectric ceramic system. *Ceram. Int.*, 2003, **29**(1), 35-39.
doi: 10.1016/S0272-8842(02)00086-X
 25. Cheng, S. & Hsieh, H.L. Piezoelectric properties of $\text{Pb}(\text{Ni}_{1/3}\text{Sb}_{2/3})\text{O}_3\text{-PbTiO}_3\text{-PbZrO}_3$ ceramics modified with MnO_2 additive, *J. Eur. Ceram. Soc.* 2005, **25**(12), 2425-2427.
doi: 10.1016/j.jeurceramsoc.2005.03.075
 26. Sumara, J.I. & Osak, A. Dielectric, ferroelectric and pyroelectric properties of $\text{Pb}(\text{Ni}_{1/3}\text{Sb}_{2/3}\text{Ti}_y\text{-Zr}_z\text{O}_3)$ ceramics. *Physica B: Condensed Matter.*, 2009, **404**(20), 3698-3702.
doi: 10.1016/j.physb.2009.06.062
 27. Lonkar, C.M.; Premkumar, S.; Kharat, D.K.; Kumar, H.H.; Prasad, S. & Balasubramanian, K. Behaviour of $\text{Pb}(\text{Ni}_{1/3}\text{Sb}_{2/3})\text{O}_3\text{-Pb}(\text{ZrTi})\text{O}_3$ ferroelectric ceramics under cyclic electric loading. *J. Mater. Sci. Mater. Electron.*, 2013, **24**(6), 1989-1993.
doi: 10.1007/s10854-012-1046-5
 28. Kumar, M.; Rao, T.N.; Jagadisan, K Rao, K.J. Tailoring of vibration test specifications for a flight vehicle. *Def. Sci. J.*, 2002, **52**(1), 41-45.
doi: 10.14429/dsj.52.2147
 29. International Centre for Diffraction Data. ICDD-00-026-0142.
 30. International Centre for Diffraction Data. ICDD-01-070-4258.
 31. International Centre for Diffraction Data. ICDD-01-070-4844.
 32. International Centre for Diffraction Data. ICDD-74-1354
 33. Wang, M.C.; Huang, M.S. & Nan-Chung, W. Low-temperature sintering of $12\text{Pb}(\text{Ni}_{1/3}\text{Sb}_{2/3})\text{O}_3\text{-}40\text{PbZrO}_3\text{-}48\text{PbTiO}_3$ with V_2O_5 and excess PbO additives. *J. Eur. Ceram. Soc.*, 2002, **22**(5), 697 - 705.
doi: 10.1016/S0955-2219(01)00374-0
 34. Kong, L.B.; Zhu, W. & Tan, O.K. Preparation and characterization of $\text{Pb}(\text{Zr}_{0.52}\text{Ti}_{0.48})\text{O}_3$ ceramics from high-energy ball milling powders. *Mater. Lett.* 2000, **42**(4), 232-239.
doi: 10.1016/S0167-577X(99)00190-1
 35. Kungl, H. & Michael, J. Effects of sintering temperature on microstructure and high field strain of niobium-strontium doped morphotropic lead zirconatetitanate. *J. Appl. Phys.*, 2010, **107**(5), 054111.
doi: 10.1063/1.3294648
 36. Lu, P.W.; Xue, W.R. & Huebner, W. A Study of the sintering mechanism of PZT based piezoceramics. *IEEE*, 1995, 122–125.
doi: 10.1016/S0272-8842(01)00078-5
 37. Chen, M.; Yao, X.; & Zhang, L. Grain Size dependence of dielectric and field induced strain properties of chemically prepared $(\text{Pb},\text{La})(\text{Zr},\text{Sn},\text{Ti})\text{O}_3$ anti-ferroelectric ceramics. *Ceram. Int.*, 2002, **28**(2), 201–07.
 38. Mohammadi, F.; Khan, A. & Cass, R.B. Power Generation from piezoelectric lead zirconate titanate fiber composites. In Proceedings of the Material Research Society Symposium, 2003, **736**, D5.5.1-D5.5.6.
 39. Yamashita, Y.; Hosono, Y.; Harada, K. & Yasuda, N. Present and future of piezoelectric single crystals and the importance of B-site cations for high piezoelectric response. *IEEE Ultrason. ferr.*, 2002, **49**(2), 184-192.
 40. Vittayakorn, N.; Rujijanagul, G.; Tan, X.; Marquardt, M.A. & Cann, D.P. The morphotropic phase boundary and dielectric properties of the $x\text{Pb}(\text{Zr}_{1/2}\text{Ti}_{1/2})\text{O}_3\text{-(1-x)}\text{Pb}(\text{Ni}_{1/3}\text{Nb}_{2/3})\text{O}_3$ perovskite solid solution. *J. Appl. Phys.*,

2004, **96**(9), 5103-5109.

doi: 10.1063/1.1796511

41. Beeby, S.P.; Tudor, M.J. & White, N.M. Energy harvesting vibration sources for microsystems applications. *Meas. Sci. Technol.*, 2006. **17**(12), R175–R195.
doi: 10.1088/0957-0233/17/12/R01
42. Umeda, M.; Nakamura, K. & Ueha, S. Energy storage characteristics of a piezoelectric generator using impact vibration. *Jpn. J. App. Phys.*, 1997, **36**(1), 3146–3151.
doi: 10.1143/JJAP.36.3146
43. Kyriassis, J.; Kendall, C.; Paradiso, J. & Gershenfeld, N. Parasitic power harvesting in shoes. In 2nd IEEE International Conference on Wearable Computing 1998, 132-39.
44. Green, C.; Mossi, K.M. & Bryant, R.G. Scavenging energy from piezoelectric materials for wireless sensor applications. In Proceedings of IMECE2005 2005, ASME International Mechanical Engineering Congress and Exposition, IMECE2005 80426, Orlando, Florida USA, (November 5-11, 2005).
doi: 10.1115/imece2005-80426

ACKNOWLEDGEMENTS

Authors would like to thank Director, Armament Research and Development Establishment (ARDE), Pune and Vice Chancellor, Defence Institute of Advanced Technology (DIAT), Pune for encouragement and permission to publish the paper. We express our sincere thanks to Dr Ashutosh Abhyankar, Dr Himanshu Panda and their team at DIAT for their support for HRTEM and FESEM. Authors are also thankful to the colleagues at PZT Centre for fabrication of piezo material. Thanks are also due to colleagues of Range and Instrumentation Division of ARDE for providing vibration facility. We are thankful to M/s Vibration Research, Hyderabad for collection and processing of vibration data.

CONTRIBUTORS

Mr H.H. Kumar received his MSc (Physics) from Pune University, in 1984. Presently, working as Scientist ‘G’ at ARDE, Pune. He has 37 research publications in peer reviewed journals, over 70 publications in seminars and conferences, one book chapter and three patents to his credit. His main areas of research are ferroelectric materials, nano materials, lead free piezo materials and energy harvesting devices for strategic applications.

Dr C.M. Lonkar received the MSc (Physics) from Pune University and PhD (Materials Science) from Defence Institute of Advanced Technology, Pune. Presently, working at ARDE, Pune. He has 16 publications in peer reviewed journals/conferences, one book chapter and filing of a patent to his credit. His main areas of research interest are development of ferroelectric materials and devices for strategic and emerging technological applications. Currently, he is working on Nano PZT based materials, composites and devices for power harvesting and sensor applications.

Prof. Balasubramanian K. is Dean (Academics) and Professor/Head of Materials Engineering at Defence Institute of Advanced Technology, Pune. He has over 80 research papers in peer reviewed journal and over 200 conference/invited talks. He was awarded the Prestigious Best Researcher of the Year, 2014 by the Ministry of Defence, Government of India, for outstanding contribution and development of ‘novel hybrid ablative composite as thermal; Protection systems for re-entry vehicles’.